Acta Crystallographica Section C
Crystal Structure Communications
ISSN 0108-2701

The isothiocyanate complex of triphenylborane forms an unusual coordination polymer with $[K(18\text{-crown-}6)]^+$, both in the solid state and in solution

Orde Q. Munro* and Nicole Pearson

School of Chemical and Physical Sciences, University of Natal, Private Bag X01, Scottsville 3209, Pietermaritzburg, South Africa
Correspondence e-mail: munroo@nu.ac.za

Received 8 July 2003
Accepted 14 August 2003
Online 23 September 2003

The title salt, (1,4,7,10,13,16-hexaoxacyclooctadecane-κ^6O)-[(isothiocyanato)triphenylborato-κ*S*]potassium(I), $[K(C_{19}H_{15}BNS)(C_{12}H_{24}O_6)]$ or $[K(SCNBPh_3)(18\text{-crown-}6)]$, where 18-crown-6 is 1,4,7,10,13,16-hexaoxacyclooctadecane and $[SCNBPh_3]^-$ is the (isothiocyanato)triphenylborate anion, exhibits a supramolecular structure that is best described as a helical coordination polymer or molecular screw. This unusual supramolecular structure is based on a framework in which the SCN^- ion bridges the chelated K^+ ion and the B atom of BPh_3 in a μ_2 fashion. The X-ray crystal structure of the title salt has been determined at 100 (1) and 293 (2) K. The K^+ ion exhibits axial ligation by the S atom of the $[SCNBPh_3]^-$ anion, with a K—S distance of 3.2617 (17) Å (100 K). The *trans*-axial ligand is an unexpected η^2-bound C═C bond of a phenyl group (*meta*- and *para*-C atoms) that belongs to the BPh_3 moiety of a neighboring molecule. The K—C bond distances span the range 3.099 (3)–3.310 (3) Å (100 K) and are apparently retained in $CDCl_3$ solution (as evidenced by ^{13}C NMR spectroscopy). By virtue of the latter interaction, the supramolecular structure is a helical coordination polymer, with the helix axis parallel to the *b* axis of the unit cell. IR spectroscopy and semi-empirical molecular orbital (AM1) calculations have been used to investigate further the electronic structure of the $[SCNBPh_3]^-$ ion.

Comment

The thiocyanate ion is a well known ambidentate ligand that can coordinate to metal ions through the N (Sudbrake & Vahrenkamp, 2001) or the S atom (Nelson *et al.*, 1982; Uttecht & Preetz, 2001). This property also favors the formation of dimeric and polymeric structures (Rudolph & Hartl, 1997; Zhang *et al.*, 1997) in which the SCN^- ion bridges identical or inequivalent metal ions to give homobimetallic (*M*—S—C≡N—*M*) and heterobimetallic (*M*—S—C≡N—*M*′) systems (Harrowfield *et al.*, 1996; Labahn *et al.*, 1999). Since the N atom is a harder ligand donor than the S atom [Pearson's classification of hard and soft bases (Pearson, 1963)], it is reasonable to assume that a soft metal ion, *e.g.* a 5*d* or sixth-row main-group metal in a low oxidation state, would favor coordination to thiocyanate *via* the S atom (Drew *et al.*, 1978). In contrast, hard metal ions would be expected to prefer coordination to the harder N-donor and thus favor the formation of N-bound isothiocyanate complexes (Pohl *et al.*, 1987). While these assumptions appear to be correct for many complexes, metal ions with an intermediate hard/soft character are clearly faced with two options as far as coordination to SCN^- is concerned, with both *N*- and *S*-coordination to the same metal ion being found in several interesting cases (Nelson *et al.*, 1982; Zhu *et al.*, 2001). The fundamental question, therefore, is whether it is possible to control the manner in which thiocyanate binds to metal ions that are moderately soft.

We have recently begun an investigation of the structures and coordination chemistry of thiocyanate complexes of five- and six-coordinate Fe^{III} and Co^{III} porphyrins in an effort to understand the factors that govern linkage isomerism and linear *versus* bent coordination of the SCN^- ion in these systems (Pearson, 2002). During the course of this work, we realized that one way to control the delivery of the SCN^- ion to the metal binding site is to tie up one of the donor atoms using the guiding principles of hard/soft acid/base (HSAB) theory, namely that the N atom of the SCN^- ion is hard and can therefore be captured by a hard Lewis acid prior to delivery to the target metal ion (Co^{III} in the case of our work on porphyrins). In this paper, we show that triphenylborane (BPh_3) is an easily handled Lewis acid that is well suited (although it is sterically bulky) to a role as an N-atom blocking group for the SCN^- ion.

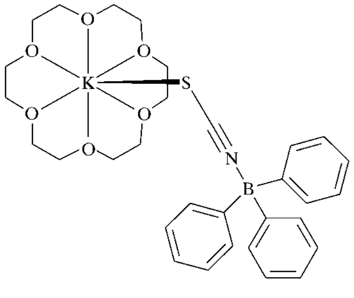

(I)

Selected structural parameters of the title compound, (I), at 100 (1) and 293 (2) K are given in Tables 1 and 2, respectively. The following discussion pertains to the low-temperature data unless otherwise indicated. The ambidenticity of the SCN^- ion is confirmed in Fig. 1(*a*), which clearly shows that the anion is axially coordinated to the K^+ ion within the crown through the S atom and to the B atom of BPh_3 through the N atom. The S1—K1 axial coordination interaction is characterized by a relatively long bond of 3.2617 (17) Å. However, since this is some 1.3 Å shorter than the sum of the van der Waals radii of the two bonded elements (4.55 Å), it is clearly a formal coordination interaction. The S1—K1 distance in (I) compares favorably with that reported for the Yb^{III} derivative *catena*-bis(μ_2-thiocyanato-κ^2N,S)(18-crown-6)potassium bis(η^5-pentamethylcyclopentadienyl)ytterbium(III) [3.226 (2) Å; Labahn *et al.*, 1999]. The N1—B1 bond length, on the other hand, is 1.567 (3) Å, and this is evidently a more regular dative covalent bond, particularly if we consider the mean B—C bond distance [1.636 (5) Å]. The mean K—O coordination distance is 2.80 (4) Å; the large s.u. of the mean arises from the broad range [2.7666 (15)–2.8651 (15) Å; Table 1]. The mean *cis*-O—K—O and *trans*-O—K—O bond angles are 60.1 (6) and 167.9 (9)°, respectively. The marked deviation of the latter angle from 180° reflects the sizeable out-of-plane displacement of the K$^+$ ion towards the axial S atom (see below).

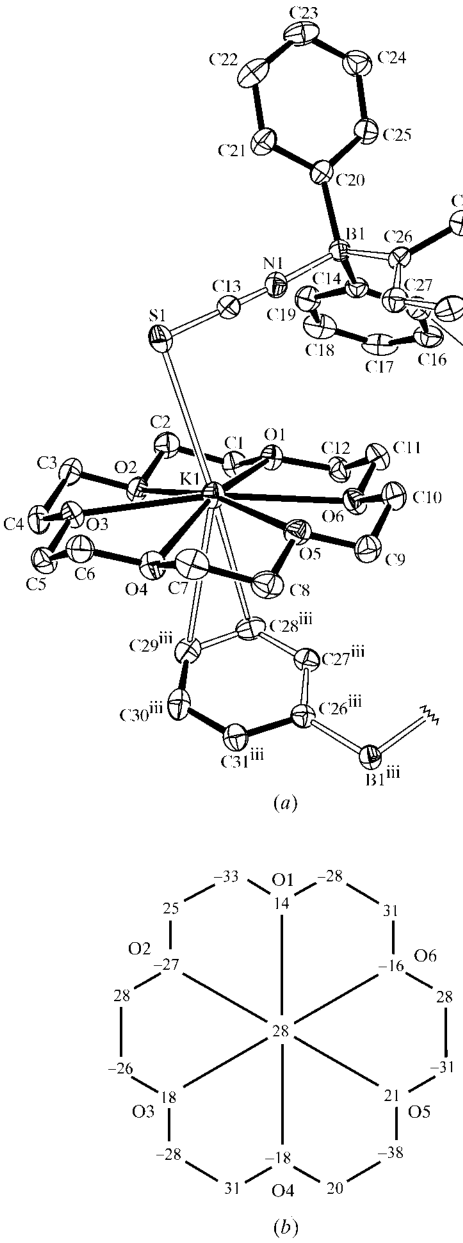

(*a*)

(*b*)

Figure 1
(*a*) Labeled view of (I) (60% probability displacement ellipsoids, 100 K). All H atoms have been omitted for clarity. The axial ligand *trans* to the S-bound [SCNBPh$_3$]$^-$ ion is the phenyl ring of a neighboring [SCNBPh$_3$]$^-$ ion. Open bonds link atoms that constitute the backbone of the helical coordination polymer. [Symmetry code: (iii) $-x, y+\frac{1}{2}, -z+\frac{1}{2}$.] (*b*) Formal diagram of the conformation of the [K(18-crown-6)]$^+$ cation, showing the perpendicular displacements [in units of 0.010 (2) Å] of each atom from the 19-atom mean plane.

The 18-crown-6 macrocycle has a conformation not unlike the teeth of a cylindrical saw, with the ring atoms alternately displaced above and below the mean plane of the [K(18-crown-6)]$^+$ ion (Fig. 1*b*). The maximum and minimum perpendicular atomic displacements from the mean plane of the macrocycle and K$^+$ ion are –0.3810 (19) (for atom C8) and 0.1352 (13) Å (for atom O1), respectively. The K$^+$ ion is displaced towards the axial S atom by 0.2829 (6) Å and the mean value of the absolute perpendicular atomic displacements from the 19-atom mean plane is a substantial 0.26 (6) Å.

Coordination of the S atom of [SCNBPh$_3$]$^-$ to the K$^+$ ion of [K(18-crown-6)]$^+$ is characterized by an unexpectedly narrow K1—S1—C13 angle of 94.98 (7)°. (The K—S—C angles in two other potassium thiocyanate derivatives are ~120°; Labahn *et al.*, 1999; Habata *et al.*, 2000.) Furthermore, the axial K1—S1 bond is substantially tilted from the normal to the mean plane of the metallated crown ether. This tilt is clearly evident from the O—K—S angles given in Table 1, which span a broad range from 78.98 (3) (for O3—K1—S1) to 111.48 (3)° (for O6—K1—S1), and from the view of (I) shown in Fig. 1(*a*). The origin of this marked structural distortion can be traced to the unexpected coordination of an aryl ring C atom to the potassium ion (*trans* to atom S1) from a neighboring molecule in the unit cell. The K1—C28^{iii} distance [symmetry code: (iii) $-x, y+\frac{1}{2}, -z+\frac{1}{2}$] is 3.099 (3) Å and is therefore considerably shorter than the K1—S1 bond, even though the K$^+$ ion is displaced towards the S atom. Moreover, since the K1—C29^{iii} distance is 3.310 (3) Å, the K$^+$ ion effectively shows asymmetric η^2-type coordination to a C=C bond of the neighboring aryl ring. Organometallic complexes of potassium metal or K$^+$ that exhibit both η^1- and η^2-coordination are well known (Kuhl *et al.*, 1999; Chitsaz & Neumuller, 2001; Ganesan

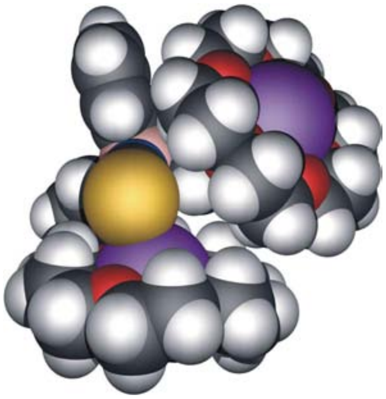

Figure 2
Space-filling plot (CPK model) of (I), illustrating the off-axis tilt of the axial [SCNBPh$_3$]$^-$ ion caused by steric interactions resulting from coordination of one of the BPh$_3$ phenyl rings to the neighboring [K(18-crown-6)]$^+$ cation.

et al., 2002); the K—C distances are typically in the range 2.9–3.5 Å. Inspection of the Cambridge Structural Database (Allen, 2002) reveals that potassium readily forms organometallic complexes with coordination numbers as high as η^8 to a single ligand in the case of bicyclic aromatic species (Cloke *et al.*, 2000) or the cyclooctatetraenyl anion (Xia *et al.*, 1991).

The *trans*-S1—K1—C28$^{\rm iii}$ bond angle [159.10 (4)°] deviates significantly from 180° because of the close proximity of the crown ether to which atoms C28 and C29 are bound (Fig. 2). Steric repulsion between the neighboring crown ethers evidently requires that the K1—S1 bond and $[SCNBPh_3]^-$ ion tilt away from the vector perpendicular to the mean plane of the cation in order to minimize unfavorable cation–cation and cation–anion non-bonded contacts. A useful descriptor of the lateral axial ligand displacement is the dihedral angle between the mean plane of the metallated crown ether and the triad K1—S1—C13, which is 71.75 (5)°. Interestingly, the ^{13}C NMR spectrum of (I) showed two distinct *meta*- and *para*-carbon signals for the BPh_3 phenyl groups, strongly suggesting that the K1—C28/C29 η^2-coordination interaction observed in the solid state is also maintained in solution.

Inspection of the bond distances for (I) listed in Table 1 confirms that the thiocyanate ion has a Lewis structure that is fully consistent with a single bond between the S and C atoms and a C≡N triple bond. Furthermore, the S1—C13—N1—B1 tetrad is essentially linear, with the two bond angles subtended at atoms C13 and N1 falling within 5° of 180°. The assigned resonance form for the SCN^- ion in this system is confirmed by the IR stretching frequencies for (I) (2160 cm^{-1} for the C≡N bond and 840 cm^{-1} for the C—S bond), which are typical of the values expected for such bonds (Nakamoto, 1986). Interestingly, the C≡N bond stretching frequency is shifted by 106 cm^{-1} to a higher wavenumber relative to [K(16-crown-6)(SCN)] upon coordination to BPh_3. This shift reflects σ-electron donation from the N atom to a Lewis acid that is incapable of π-backbonding with the unsaturated ligand. Ultimately, an increase in polarity of the C≡N bond upon formation of the N—B bond results in the observed increase in the vibrational frequency. The key question is by how much does the electronic structure of the SCN^- ion change with the addition of BPh_3. Before we answer this question with semi-empirical molecular orbital calculations (AM1; Dewar *et al.*, 1985), it is noteworthy that the opposite appears to be true for the C—S bond, since the formation of complex (I) results in a small (7 cm^{-1}) shift to lower wavenumber for the ν(CS) mode.

AM1 is parameterized for all of the elements present in (I) except K. Since our main objective in this work was to capture the N atom of the SCN^- ion by coordination to boron, we have elected to focus on what effect B—N bond formation has on the electronic structure of the thiocyanate ion. The *in vacuo* AM1-calculated Mulliken charge distribution for $[SCNBPh_3]^-$ is shown in Fig. 3(*a*) and that for the SCN^- ion is given in Fig. 3(*b*). As implied by the change in the experimental vibrational frequency of the C≡N bond, the calculated charge distribution for the $[SCNBPh_3]^-$ ion is consistent with marked polarization of the electron density by the B atom. Specifically, the partial negative charge on the N atom drops to 67% of its value in the free SCN^- ion upon coordination to boron. The fractional charge on the S atom decreases to $\sim$54° of its value in SCN^-. However, both of these changes are dwarfed by the drop in the partial negative charge for the central C atom from −0.161 to −0.028 e (*i.e.* to 17% of its value in the free SCN^- ion). More important is the fact that the S—C and C≡N bonds become more polar when the SCN^- ion binds to BPh_3. For example, the partial charge difference for the C≡N bond increases from 0.161 to 0.188 e on going from SCN^- to $[SCNBPh_3]^-$. In principle, stronger electrostatic attraction between the bonded atoms should increase the vibrational frequencies for the bonds constituting the SCN^- ion.

It transpires that some useful information can be gleaned from the *in vacuo* AM1-calculated structures of the SCN^- and $[SCNBPh_3]^-$ ions. First, the calculated S—C (1.53 Å), C—N (1.18 Å), and N—B (1.53 Å) bond lengths of $[SCNBPh_3]^-$ compare favorably with those determined experimentally for (I) (Table 1), even though the [K(18-crown-6)]$^+$ ion was not included in the calculations. Secondly, the calculated S—C and C—N bond distances for the free SCN^- ion (1.57 and 1.18 Å, respectively) reveal that coordination to BPh_3 slightly increases the bond order, particularly of the C—S bond. The calculated vibrational frequencies are thus higher for $[SCNBPh_3]^-$ [ν(C≡N) = 2385 cm^{-1} and ν(C—S) = 855 cm^{-1}] than for SCN^- [ν(C≡N) = 2372 cm^{-1} and ν(C—S) = 801 cm^{-1}]. The calculated frequency change for the C≡N bond is smaller than that observed experimentally, whereas that for the C—S bond is larger and in the opposite direction. We surmise that these discrepancies probably reflect the omission of the [K(18-crown-6)]$^+$ ion from the simulations (particularly the S—K$^+$ coordination interaction) and the relatively low level of theory inherent in the AM1 model. [We are currently running density functional theory (DFT) simulations on the present SCN^- system, as well as the thiocyanate

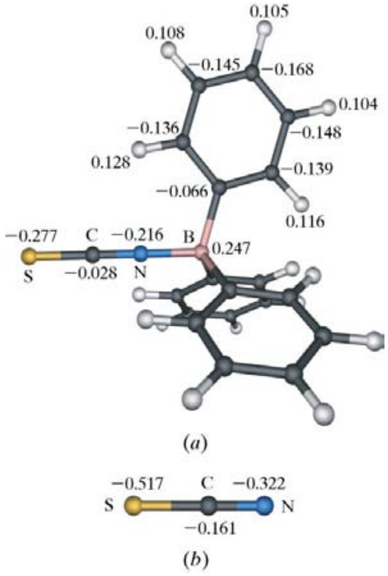

Figure 3
AM1-calculated Mulliken charges for (*a*) $[SCNBPh_3]^-$ and (*b*) SCN^-.

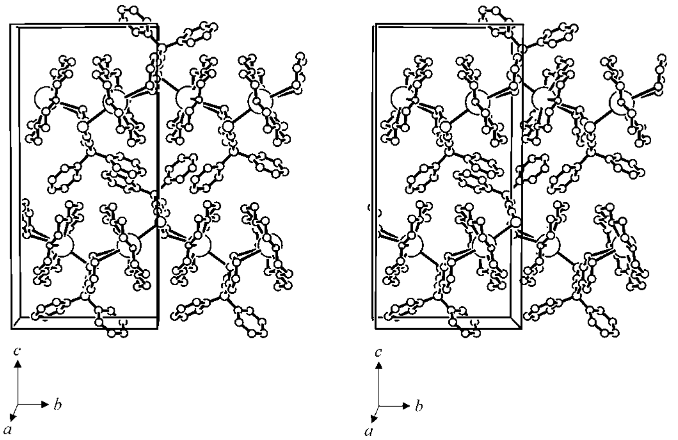

Figure 4
A stereoview (*PLUTON*; Spek, 1991) of selected contents of two neighboring unit cells of (I), viewed approximately along the crystallographic *a* axis.

and isothiocyanate complexes of a range of metalloporphyrins, in order to further elucidate the electronic structures of the SCN^- ion in these species.]

The unit cell of (I) comprises four molecules (Fig. 4). As noted above, the somewhat unexpected coordination interaction between each K^+ ion and the C=C bond of a neighboring BPh_3 moiety leads to the formation of a helical polymer with an axis running parallel to the *b* axis of the unit cell, *i.e.* parallel to the vector joining adjacent K^+ ions in the lattice. The coordination polymer can be formulated very simply by designation of its repeat unit, *viz.* $\{[K(18\text{-crown-}6)][SCNBPh_3]\}_n$. The significance of the chiral space group becomes more apparent upon inspection of the supramolecular structure of (I). Specifically, the polymer backbone, which includes the K^+ ions and the ligand donor atoms S and C, is seen to spiral in a corkscrew fashion from left to right in a counterclockwise direction. Although we did not experimentally determine the absolute configuration of the crystal specimen used for the X-ray diffraction study, the left-handed helicity of the polymer chain is correct according to the Flack (1983) absolute structure parameter. (The bulk material is, of course, racemic.) Finally, it is noteworthy that other coordination polymers with bridging thiocyanate ions also crystallize in the chiral space group $P2_12_12_1$ (Hehl & Thiele, 2000). A second, somewhat earlier, example is the copper(I) coordination polymer *catena*-(μ_2-thiocyanato)bis(quinoline)-copper(I) (Healy *et al.*, 1984).

Experimental

All manipulations were carried out under nitrogen using a double manifold vacuum line, Schlenkware and cannula techniques. Tetrahydrofuran (THF) and hexane were distilled over sodium/benzophenone, and dichloromethane (CH_2Cl_2) was distilled over CaH_2. Triphenylborane, 18-crown-6 (1,4,7,10,13,16-hexaoxacyclooctadecane) and KSCN (Aldrich) were used as received. The following locally developed method was used to synthesize [K(18-crown-6)-(SCN)]. To 18-crown-6 (10 g, 37.8 mmol) and KSCN (7.35 g, 75.6 mmol) in a 100 ml two-necked round-bottomed flask under nitrogen was added freshly distilled THF (100 ml). The solution was stirred under nitrogen overnight. The product was filtered *via* cannula methods into a second (dry) round-bottomed flask prior to slow addition of dry hexane to induce crystallization of the product. IR (cm^{-1}, KBr pellet): 2054 [*s*, $\nu(C\equiv N)$], 847 [*m*, $\nu(C-S)$], 464 [*w*, $\delta(N\equiv C-S)$]. To triphenylborane (1.5 g, 6.17 mmol) and [K(18-crown-6)(SCN)] (1.49 g, 4.11 mmol) in a 100 ml two-necked round-bottomed flask under nitrogen was added freshly distilled CH_2Cl_2 (100 ml). The solution was stirred under nitrogen for 4 h prior to cannula filtration into a second round-bottomed flask under nitrogen. Dry hexane was added slowly in order to crystallize the product, *viz.* $[K(18\text{-crown-}6)(SCNBPh_3)]$ (isolated yield 1.66 g, 67%). A 12 mg portion was redissolved in freshly distilled CH_2Cl_2 (2.5 ml), transferred into a 18 × 180 mm Schlenk tube and layered with hexane. X-ray quality crystals were obtained after 8 d. IR (cm^{-1}, KBr pellet): 2160 [*s*, $\nu(C\equiv N)$], 840 [*m*, $\nu(C-S)$], 470 [*w*, $\delta(N\equiv C-S)$]; ^1H NMR (499.98 MHz, $CDCl_3$, p.p.m.): 7–7.4 (*m*, 15H, Ar–H), 3.47 (*s*, 12H, crown-CH_2); ^{13}C NMR (125.736 MHz, $CDCl_3$, p.p.m.): 69.92 (CH_2, 18-crown-6), 123.61 (*o*-C, BPh_3), 125.35, 126.25, 126.97, 131.35 (*m*- and *p*-C, BPh_3), 133.41 (α-C, BPh_3), 156.03 (C, NCS). AM1 geometry optimization calculations on SCN^- and $[SCNBPh_3]^-$ were carried out with the default singlet-state parameters in *HyperChem* (Hypercube, 2000).

Low-temperature structure

Crystal data

$[K(C_{19}H_{15}BNS)(C_{12}H_{24}O_6)]$
$M_r = 603.6$
Orthorhombic, $P2_12_12_1$
$a = 11.034$ (4) Å
$b = 11.582$ (9) Å
$c = 24.149$ (7) Å
$V = 3086$ (3) Å^3
$Z = 4$
$D_x = 1.299$ Mg m^{-3}
Mo $K\alpha$ radiation
Cell parameters from 285 reflections
$\theta = 4.2$–31.7°
$\mu = 0.28$ mm^{-1}
$T = 100$ (1) K
Rhomb, colorless
0.53 × 0.33 × 0.22 mm

Data collection

Oxford Diffraction Xcalibur2 CCD diffractometer
ω–2θ scans
Absorption correction: numerical (*CrysAlisRED*; Oxford Diffraction, 2003)
$T_{\min} = 0.810$, $T_{\max} = 0.900$
28 274 measured reflections
9621 independent reflections
8301 reflections with $I > 2\sigma(I)$
$R_{\rm int} = 0.048$
$\theta_{\max} = 31.7°$
$h = -16 \rightarrow 15$
$k = -11 \rightarrow 17$
$l = -35 \rightarrow 35$

Refinement

Refinement on F^2
$R(F) = 0.047$
$wR(F^2) = 0.095$
$S = 1.08$
9621 reflections
370 parameters
H-atom parameters constrained
$w = 1/[\sigma^2(F_o^2) + (0.0276P)^2 + 1.8032P]$ where $P = (F_o^2 + 2F_c^2)/3$
$(\Delta/\sigma)_{\max} = 0.001$
$\Delta\rho_{\max} = 0.48$ e Å^{-3}
$\Delta\rho_{\min} = -0.40$ e Å^{-3}
Absolute structure: Flack (1983), 3844 Friedel pairs
Flack parameter = 0.08 (3)

Room-temperature structure

Crystal data

$[K(C_{19}H_{15}BNS)(C_{12}H_{24}O_6)]$
$M_r = 603.6$
Orthorhombic, $P2_12_12_1$
$a = 11.0652$ (15) Å
$b = 11.7696$ (19) Å
$c = 24.424$ (4) Å
$V = 3180.8$ (8) Å^3
$Z = 4$
$D_x = 1.26$ Mg m^{-3}
Mo $K\alpha$ radiation
Cell parameters from 25 reflections
$\theta = 2$–12°
$\mu = 0.28$ mm^{-1}
$T = 293$ (2) K
Rhomb, colorless
0.53 × 0.33 × 0.22 mm

Table 1
Selected geometric parameters (Å, °) for the low-temperature structure.

C20—B1	1.641 (3)	K1—O3	2.7911 (16)
C26—B1	1.632 (3)	K1—O5	2.7966 (15)
C13—N1	1.154 (2)	K1—O6	2.8312 (16)
C13—S1	1.6282 (19)	K1—O2	2.8651 (15)
C14—B1	1.634 (3)	K1—C28^{i}	3.099 (3)
B1—N1	1.567 (3)	K1—S1	3.2617 (17)
K1—O4	2.7666 (15)	K1—C29^{i}	3.310 (3)
K1—O1	2.7687 (15)		
C29—C28—K1^{ii}	86.39 (11)	O5—K1—C28^{i}	88.98 (5)
C27—C28—K1^{ii}	113.15 (12)	O6—K1—C28^{i}	70.82 (5)
C30—C29—K1^{ii}	120.82 (13)	O2—K1—C28^{i}	78.62 (5)
C28—C29—K1^{ii}	69.12 (11)	O4—K1—S1	104.68 (4)
N1—C13—S1	179.7 (2)	O1—K1—S1	87.20 (5)
N1—B1—C26	106.98 (14)	O3—K1—S1	78.98 (3)
N1—B1—C14	106.96 (14)	O5—K1—S1	110.46 (4)
N1—B1—C20	106.98 (14)	O6—K1—S1	111.48 (3)
O4—K1—O1	167.35 (4)	O2—K1—S1	82.16 (5)
O4—K1—O3	60.13 (4)	C28^{i}—K1—S1	159.10 (4)
O4—K1—O5	60.97 (5)	O4—K1—C29^{i}	73.73 (5)
O1—K1—O6	59.16 (4)	O1—K1—C29^{i}	93.83 (6)
O3—K1—O6	168.84 (4)	O3—K1—C29^{i}	74.51 (5)
O5—K1—O6	60.37 (4)	O5—K1—C29^{i}	95.08 (5)
O1—K1—O2	60.31 (4)	O6—K1—C29^{i}	94.39 (5)
O3—K1—O2	59.52 (4)	O2—K1—C29^{i}	72.59 (5)
O5—K1—O2	167.36 (4)	C28^{i}—K1—C29^{i}	24.49 (5)
O4—K1—C28^{i}	91.23 (5)	S1—K1—C29^{i}	150.06 (4)
O1—K1—C28^{i}	76.21 (5)	C13—N1—B1	174.41 (18)
O3—K1—C28^{i}	98.01 (5)	C13—S1—K1	94.98 (7)
O4—K1—S1—C13	148.19 (7)	O6—K1—S1—C13	18.99 (8)
O1—K1—S1—C13	−36.20 (7)	O2—K1—S1—C13	−96.60 (8)
O3—K1—S1—C13	−156.95 (7)	C28^{i}—K1—S1—C13	−73.37 (13)
O5—K1—S1—C13	84.14 (8)	C29^{i}—K1—S1—C13	−129.01 (10)

Symmetry codes: (i) $2-x, y-\frac{1}{2}, \frac{1}{2}-z$; (ii) $2-x, \frac{1}{2}+y, \frac{1}{2}-z$.

Table 2
Selected geometric parameters (Å, °) for room-temperature structure.

C20—B1	1.638 (3)	K1—O4	2.7651 (17)
C26—B1	1.627 (3)	K1—O3	2.7784 (16)
C28—K1^{ii}	3.174 (2)	K1—O5	2.8010 (17)
C29—K1^{ii}	3.394 (3)	K1—O6	2.8156 (17)
C13—N1	1.150 (3)	K1—O2	2.8602 (17)
C13—S1	1.617 (2)	K1—C28^{i}	3.174 (2)
C14—B1	1.626 (3)	K1—S1	3.3064 (10)
B1—N1	1.568 (3)	K1—C29^{i}	3.394 (3)
K1—O1	2.7604 (16)		
C29—C28—K1^{ii}	87.92 (14)	O5—K1—C28^{i}	89.47 (5)
C27—C28—K1^{ii}	112.40 (14)	O6—K1—C28^{i}	72.48 (6)
C28—C29—K1^{ii}	69.16 (14)	O2—K1—C28^{i}	78.82 (5)
C30—C29—K1^{ii}	121.56 (16)	O1—K1—S1	87.53 (4)
N1—C13—S1	179.3 (2)	O4—K1—S1	103.74 (4)
N1—B1—C14	106.59 (17)	O3—K1—S1	80.20 (4)
N1—B1—C26	107.02 (17)	O5—K1—S1	108.49 (4)
N1—B1—C20	107.22 (17)	O6—K1—S1	110.02 (4)
O1—K1—O4	168.06 (5)	O2—K1—S1	83.39 (4)
O4—K1—O3	60.04 (5)	C28^{i}—K1—S1	160.79 (5)
O4—K1—O5	60.86 (5)	O1—K1—C29^{i}	94.09 (6)
O1—K1—O6	59.53 (5)	O4—K1—C29^{i}	74.11 (6)
O3—K1—O6	169.26 (5)	O3—K1—C29^{i}	74.90 (6)
O5—K1—O6	60.34 (5)	O5—K1—C29^{i}	94.72 (6)
O1—K1—O2	60.09 (5)	O6—K1—C29^{i}	94.40 (6)
O3—K1—O2	59.57 (5)	O2—K1—C29^{i}	73.65 (5)
O5—K1—O2	168.10 (5)	C28^{i}—K1—C29^{i}	22.92 (6)
O1—K1—C28^{i}	77.36 (6)	S1—K1—C29^{i}	152.28 (5)
O4—K1—C28^{i}	90.79 (6)	C13—N1—B1	175.3 (2)
O3—K1—C28^{i}	96.78 (6)	C13—S1—K1	96.95 (9)
O1—K1—S1—C13	−34.98 (10)	O6—K1—S1—C13	21.25 (10)
O4—K1—S1—C13	149.02 (10)	O2—K1—S1—C13	−95.14 (10)
O3—K1—S1—C13	−155.31 (10)	C28^{i}—K1—S1—C13	−72.87 (18)
O5—K1—S1—C13	85.56 (10)	C29^{i}—K1—S1—C13	−129.08 (13)

Symmetry codes: (i) $2-x, y-\frac{1}{2}, \frac{1}{2}-z$; (ii) $2-x, \frac{1}{2}+y, \frac{1}{2}-z$.

Data collection

Enraf–Nonius CAD-4 diffractometer
Non-profiled $\omega/2\theta$ scans
13 000 measured reflections
5586 independent reflections
4976 reflections with $I > 2\sigma(I)$
$R_{\rm int} = 0.027$

$\theta_{\rm max} = 25.0°$
$h = -13 \rightarrow 1$
$k = -13 \rightarrow 13$
$l = -29 \rightarrow 29$
3 standard reflections
every 143 reflections
intensity decay: 11%

Refinement

Refinement on F^2
$R(F) = 0.032$
$wR(F^2) = 0.094$
$S = 1.07$
5586 reflections
370 parameters
H-atom parameters constrained

$w = 1/[\sigma^2(F_o^2) + (0.0501P)^2 + 0.5418P]$
where $P = (F_o^2 + 2F_c^2)/3$
$(\Delta/\sigma)_{\rm max} = 0.03$
$\Delta\rho_{\rm max} = 0.28$ e Å^{-3}
$\Delta\rho_{\rm min} = -0.27$ e Å^{-3}
Absolute structure: Flack (1983), 2428 Friedel pairs.
Flack parameter = 0.01 (4)

A difference Fourier calculation after refinement of all non-H atoms anisotropically located most of the H atoms. However, all H atoms were treated using the standard riding model of *SHELXL*97 (Sheldrick, 1997). In the room-temperature structure of (I), rigid bond restraints (DELU command) were used for atoms C26–C31, N1, C13 and S1, since large deviations (greater than 10 s.u.) were observed for the components of the anisotropic displacement parameters in the direction of the bonds involving these atoms. The absolute configuration of the crystal studied was determined from the Flack (1983) parameter. Although we did not collect data from more than one crystal specimen, the bulk material is racemic, since the reactants are not chiral.

For (I) at 100 K, data collection: *CrysAlisCCD* (Oxford Diffraction, 2003); cell refinement: *CrysAlisRED* (Oxford Diffraction, 2003); data reduction: *CrysAlisRED*. For (I) at room temperature, data collection: *CAD*-4 *Software* (Enraf–Nonius, 1992); cell refinement: *CAD*-4 *Software*; data reduction: *PROFIT* (Streltsov & Zavodnik, 1989). For (I) at both temperatures, program(s) used to solve structure: *SHELXS*97 (Sheldrick, 1997); program(s) used to refine structure: *SHELXL*97 (Sheldrick, 1997); molecular graphics: *WinGX* (Farrugia, 1999) and *ORTEP*-3 *for Windows* (Farrugia, 1997); software used to prepare material for publication: *WinGX*.

The authors thank the University of Natal Research Fund and the National Research Foundation (Pretoria) for financial support.

Supplementary data for this paper are available from the IUCr electronic archives (Reference: JZ1569). Services for accessing these data are described at the back of the journal.

References

Allen, F. H. (2002). *Acta Cryst.* B**58**, 380–388.
Chitsaz, S. & Neumuller, B. (2001). *Organometallics*, **20**, 2338–2344.
Cloke, F. G. N., Kuchta, M. C., Harker, R. M., Hitchcock, P. B. & Parry, J. S. (2000). *Organometallics*, **19**, 5795–5798.

Dewar, M. J. S., Zoebisch, E. G., Healy, E. F. & Stewart, J. P. P. (1985). *J. Am. Chem. Soc.* **107**, 3902–3909.

Drew, M. G. B., Rodgers, A., McCann, M. & Nelson, S. M. (1978). *J. Chem. Soc. Chem. Commun.* pp. 415–416.

Enraf–Nonius (1992). *CAD*-4 *Software*. Version 1.1. Enraf–Nonius, Delft, The Netherlands.

Farrugia, L. J. (1997). *J. Appl. Cryst.* **30**, 565.

Farrugia, L. J. (1999). *J. Appl. Cryst.* **32**, 837–838.

Flack, H. D. (1983). *Acta Cryst.* A**39**, 876–881.

Ganesan, M., Berube, C. D., Gambarotta, S. & Yap, G. P. A. (2002). *Organometallics*, **21**, 1707–1713.

Habata, Y., Saeki, T., Akabori, S., Zhang, X. X. & Bradshaw, J. S. (2000). *Chem. Commun.* pp. 1469–1470.

Harrowfield, J. M., Miyamae, H., Skelton, B. W., Soudi, A. A. & White, A. H. (1996). *Aust. J. Chem.* **49**, 1127–1133.

Healy, P. C., Pakawatchai, C., Papasergio, R. I., Patrick, V. A. & White, A. H. (1984). *Inorg. Chem.* **23**, 3769–3776.

Hehl, R. & Thiele, G. (2000). *Z. Anorg. Allg. Chem.* **626**, 2167–2172.

Hypercube (2000). *HyperChem*. Version 6.03. Hypercube Inc., 1115 NW 4th Street, Gainsville, Florida 32601–4256, USA.

Kuhl, O., Sieler, J. & Hey-Hawkins, E. (1999). *Z. Kristallogr.* **214**, 496–499.

Labahn, T., Mandel, A. & Magull, J. (1999). *Z. Anorg. Allg. Chem.* **625**, 1273–1277.

Nakamoto, K. (1986). *IR and Raman Spectroscopy of Inorganic and Coordination Compounds*, 4th ed., p. 208. New York: John Wiley and Sons.

Nelson, J. H., MacDougall, J. J., Alcock, N. W. & Mathey, F. (1982). *Inorg. Chem.* **21**, 1200–1204.

Oxford Diffraction (2003). *CrysAlisCCD* and *CrysAlisRED*. Version 1.170.32 (Release 06/06/2003, *CrysAlis*170 VC++). Oxford Diffraction, Wrocław, Poland.

Pearson, N. (2002). MSc thesis, University of Natal, Pietermaritzburg, South Africa.

Pearson, R. G. (1963). *J. Am. Chem. Soc.* **85**, 3533–3539.

Pohl, K., Wieghardt, K., Nuber, B. & Weiss, J. (1987). *J. Chem. Soc. Dalton Trans.* pp. 187–192.

Rudolph, L.-N. & Hartl, H. Z. (1997). *Z. Anorg. Allg. Chem.* **623**, 687–694.

Sheldrick, G. M. (1997). *SHELXL*97 and *SHELXS*97. University of Göttingen, Germany.

Spek, A. L. (1991). *PLUTON*. University of Utrecht, The Netherlands.

Streltsov, V. A. & Zavodnik, V. E. (1989). *Sov. Phys. Crystallogr.* **34**, 824–828.

Sudbrake, C. & Vahrenkamp, H. (2001). *Inorg. Chim. Acta*, **318**, 23–30.

Uttecht, J.-G. & Preetz, W. (2001). *Z. Anorg. Allg. Chem.* **627**, 1459–1464.

Xia, J., Jin, Z. & Chen, W. (1991). *J. Chem. Soc. Chem. Commun.* pp. 1214–1215.

Zhang, H., Wang, X., Zhu, H., Xiao, W. & Teo, B. K. (1997). *J. Am. Chem. Soc.* **119**, 5463–5464.

Zhu, H., Strobele, M., Yu, Z., Wang, Z., Meyer, H.-J. & You, X. (2001). *Inorg. Chem. Commun.* **4**, 577–581.